Int. J. Plasma Environ. Sci. Technol. 17 (2023) e02004 (20pp)
International Journal of Plasma Environmental Science and Technology

Review Paper DOI: 10.34343/ijpest.2023.17.e02004

Revisiting why DBDs can generate O_3 against the thermodynamic limit

Hyun-Ha Kim[1, *], Ayman A Abdelaziz[1, 2], Yoshiyuki Teramoto[1], Tomohiro Nozaki[3], Dae-Young Kim[3], Ronny Brandenburg[4], Milko Schiorlin[4], Karol Hensel[5], Young-Hoon Song[6], Dae-Hoon Lee[6], Woo-Seok Kang[6], Akira Mizuno[1, 7]

[1] National Institute of Advanced Industrial Science and Technology (AIST), Environmental Management Research Institute, Tsukuba, Japan
[2] Assuit University, Assuit, Egypt
[3] Tokyo Institute of Technology, Tokyo, Japan
[4] Leibniz Institute for Plasma and Technology, Greifswald, Germany
[5] Comenius University, Bratislava, Slovakia
[6] Korea Institute of Machinery and Materials (KIMM), Daejeon, Korea
[7] Toyohashi University of Technology, Toyohashi, Japan

* Corresponding author: hyun-ha.kim@aist.go.jp (Hyun-Ha KIM)

Received: 20 July 2023
Revised: 7 August 2023
Accepted: 8 August 2023
Published online: 9 August 2023

Abstract

This short review provides a general perspective on ozone formation and includes a brief history of the great German inventor Werner von Siemens, who invented the prototype ozonizer. The main structure of Siemens ozonizer still serves as the de facto model in large-scale applications. This review places particular focus on the thermodynamic aspect of ozone formation in dielectric barrier discharge (DBD), which is fundamental but puzzling to newcomers in plasma chemistry. As is often mentioned in the chemistry of nonthemal plasmas, non-equilibrium reactions initiated by high-energy electrons allow for the dissociation of oxygen molecules at ambient temperature, even though it is a highly endothermic process. Once atomic oxygen is formed, it spontaneously combines with oxygen molecules to form ozone with a heat release. This elaborate coupling of the non-equilibrium with equilibrium processes, as well as exothermic and endothermic processes, makes the DBD reactor an efficient and effective method for O_3 formation against the thermodynamic limits. Understanding the interplay of these elementary processes in the DBD reactor is essential in comprehending how ozone is generated, and it sheds light on further development. This review aims to provide valuable insights into the thermodynamic mechanisms behind ozone formation and some noticeable applications of ozone, assisting newcomers in plasma chemistry to grasp the underlying principles of this crucial process.

Keywords: Ozonizer, dielectric barrier discharge (DBD), ozone, thermodynamic limit, non-equilibrium.

1. Introduction

Since the invention of the ozonizer in 1857 by von Siemens, ozone has been one of the hot topics in a wide range of applications including atmospheric chemistry, air pollution, water control, and biology. At the time of the invention, Siemens first described ozone formation as “electrolysis of the gas phase” because Schönbein reported on O_3 generation using water electrolysis a few years earlier [1]. Ozonizer has long been referred to as “silent discharge” according to the paper by Andrews and Tait in 1860 [2], while dielectric barrier discharge (DBD) gained widespread acceptance in the 1990s. Although DBD is being increasingly used in many new applications, ozone generation remains one of the most successful applications from small lab-scale ($\sim 10^1$ mg h^{-1}) to industrial scale ($\sim 10^3$ kg h^{-1}) production.

Ozone is a colorless gas at low concentrations, but it becomes visible with a blue color at concentrations higher than 10%. This blue color is associated with the Chappius bands with a peak at 600 nm. Human nose is very sensitive to ozone (> 0.1 ppm) due to its pungent odor, capable of detecting it even at levels as low as parts per trillion (ppt). Indoor air standards in most countries regulate ozone concentration below 100 ppb (0.1 ppm) in workspace. On a global scale, the ozone layer in the stratosphere absorbs the Sun's ultraviolet light and protects life on Earth's surface. The issue of ozone layer depletion, known as the "ozone hole", draw significant public attention in the 1990s and led to the Montreal Protocol agreement in 1987, which aims to halt the production and use of chlorofluorocarbon (CFC) gases [3]. Ozone at high altitude (i.e., stratospheric ozone) is sometimes called "good ozone", whereas ozone at low altitude is referred to as "bad ozone". In urban areas, a combined reaction of sunlight, VOCs (volatile organic compounds), and NO_x produces ozone at a level of 10-400 ppb, causing serious acute health effects such as respiratory and cardiovascular disease. Children, chronic asthma, and pregnant women are particularly vulnerable to health damage from ozone exposure in outdoor air. Ozone generation from indoor air cleaners [4] is another source of "bad ozone" that needs to be controlled by catalyst in most cases. Two-stage plasma catalysis is a constructive development of air cleaners equipped with ozone-killing catalysts or active carbon filters.

Applications of dielectric barrier discharge (DBD) cover a wide range of areas. In plasma actuators, DBD devices are employed on surfaces to modify the gas flow and detachment behavior, making them useful in aerodynamics, flow control, and other related fields [5−7]. Despite the adverse effects of ozone on human health, it has a long history in water treatment, and its application continues to expand [8]. Surface modification by ozone is also an ongoing example of growing interest as new materials become available and relevant application arises. For example, Pratt *et al*. [9] reported ozone molecular beam (< 15%) can selectively remove carbon from metal oxides. Control of hydrophobic or hydrophilic nature of the surface [10], surface functionalization [11], catalyst preparation [12, 13] under ambient temperature, and sterilization of biocompatible plastic or living tissue are emerging areas of ozone-based surface modification.

In this work, we present a brief history of the great inventor Werner von Siemens and a list of his revolutionary inventions, including the ozonizer based on DBDs. While there are many well-organized reviews [14−18] about DBDs covering the principles of the gas discharge and its physics, to the modeling and diagnostics, so these will not be deeply covered in this review. The main focus of this short review is to explain why DBD plasma can successfully generate ozone despite the thermodynamic limit in ozone generation. The process of converting oxygen into ozone is an endergonic process ($\Delta G > 0$), which means it does not proceed at normal conditions. A unique coupling of non-equilibrium and equilibrium processes, as well as endothermic and exothermic processes, in the DBD reactor, will be discussed to help the readers in understanding ozone generation.

2. Historical overview

2.1 Werner von Siemens

Werner von Siemens (Fig. 1) is widely regarded as one of history's most talented innovators and entrepreneurs [19, 20]. Table 1 provides an overview of Siemens' numerous inventions, many of which were the world's first electrical machines. Born in 1816, he founded the Siemens and Halske Telegraph Construction (current Siemens AG) at his age of 31 (1847). One of his notable inventions in the plasma community is the ozonizer, which has also been referred to as Siemens ozonizer, silent discharge, and recently dielectric-barrier discharge (DBD). However, despite its significance, it seems that the ozonizer holds a less prominent place among his many legendary inventions. Surprisingly, a recent biography of von Siemens, written by his descendant Nathalie von Siemens, the ozonizer is not mentioned even once [19]. It is amazing how much the invention of the dynamo has impacted our modern world. Soon after this invention, he opened the gate for practical use of e-mobility such as railway, elevator, tram, and electric car. The first electric train was demonstrated in Berlin Trade Fair in 1879 on a 300-meter circular track. Otis company installed the first passenger elevator powered by a steam engine, in E.V. Haughwout & Co. (1857), a store located on the Broadway in New York. Siemens then demonstrated the first electrical elevator in 1880 at the Mannheim Trade Exhibition with a speed of 0.5 m s^{-1}. In 1882, he even constructed the first electric car which was powered by electricity from a power line. In 1888, four years before his death, he was raised to the rank of nobility by adding "von" to his name

[21]. It is also interesting to note that Röntgen used a vacuum tube from Siemens's company to discover X-rays. The name "Siemens" is still used in the international unit (SI) for electrical conductivity, denoted by the symbol "S".

Table 1. List of historical inventions by Werner von Siemens.

Contents	Year	Remarks
Ozonizer	1857	Basically, similar to current cylindrical volume DBDs
Dynamo-electric machine	1867	Charles Wheatstone also reported in 1867
Electric railway (train)	1879	Operated by DC 150V (US Patent 322,859)
Electrical Engineering	1879	He coined the term "electrical engineering" (Elektrotechnik)
Electrical elevator	1880	Mannheim Trade Exhibition with a speed of 0.5 m s^{-1}
Electric tram	1881	Build a 2.5 km line at his own expense near Berlin
Electric car	1882	Electricity supplied from power line

Fig. 1. Werner von Siemens (1816-1892).

2.2 Dielectric barrier discharge (DBD)

The most important application of DBD is ozone generation. Technically speaking there are variety ways to generate ozone. These methods include vacuum UV (VUV), X-ray and γ-ray irradiation, electron-beam [22], water electrolysis [23, 24], and electrical discharge plasmas [15, 25−27]. However, electrical discharge plasma is considered to be the only viable method of O_3 generation to meet the quantity required in plant-scale. Fundamentals and details of DBD in terms of electrical engineering and physical diagnostic can be found in well-organized reviews [14−18, 28] so only a brief description will be given in this section. Most ozonizers adopt dielectric barrier discharge, wherein the electrodes are covered with dielectric materials at one or both sides. The presence of dielectric material prevents the transition of normal discharge into spark as long as there is no physical damage to the dielectric. As schematically shown in Fig. 2 (a), air or oxygen is passed through the gap between the electrodes, where the gas molecules are exposed to electron impacts inducing excitation, dissociation, and ionization. Discharge characteristics and chemical performance depend largely on the dielectric constant, surface conductivity, and electrode gap. Borosilicate glass tube is widely used for commercial ozonizer due to its small dielectric loss factor and low cost as well. The dielectric loss factor, the product of dielectric constant (ε_s) and dielectric loss tangential (tanδ), refers to the measure of how much energy is dissipated as heat when an electromagnetic field interacts with a dielectric material. The consideration

of loss factor explicitly explains why ferroelectric materials such as $BaTiO_3$ are not adequate for dielectric barrier of DBD for O_3 generation. Alumina has also been adopted as dielectric material in DBD due to the higher thermal conductivity of 25-30 W m^{-1} K^{-1} than borosilicate glass (1 W m^{-1} K^{-1}). Indeed, developing new materials equipped with small loss factors and high thermal conductivity for effective cooling could be a significant breakthrough for the next-generation ozonizer in the future.

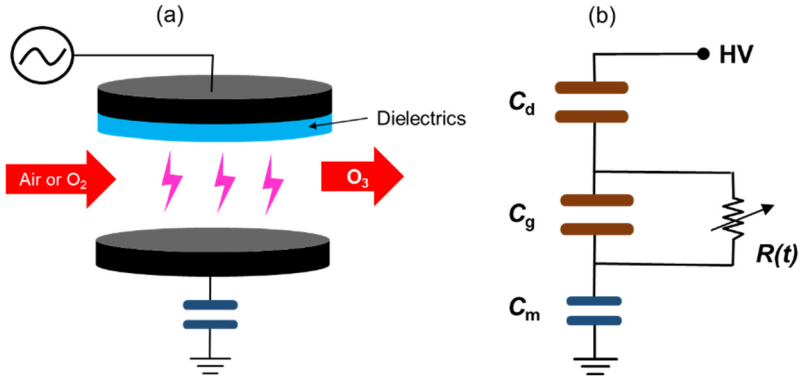

Fig. 2. Typical configuration and equivalent circuit of DBD reactor: (a) Configuration of plate-to-plate type DBD reactor (single barrier case), (b) equivalent circuit.

Ozone is one of the powerful oxidizing species that can be easily produced on-site without long-distance transformation. Table 2 summarizes the historical milestone in ozone, ozonizer, and dielectric barrier discharge. To our best knowledge, the late Louis Rosocha seems to be first coined the terminology of "dielectric barrier discharge" in 1979 [29]. "Barrier discharge" (without "dielectric") appeared sporadically in the 1960s by Jeromin [30] and 1970s by Pavlovskaya *et al*. [31] but it was not the full name of DBD. The term DBD gained widespread recognition and popularity with the milestone paper by Eliasson and Kogelschatz published in 1987 [15]. This review significantly advanced the understanding and applications of DBDs, and their paper became a key reference in the field.

Table 2. Historical milestones in ozone and ozonizer [1, 2, 27].

Year	Researcher/ Location	Remarks
1785	van Marum	Noticed ozone smell near static machine. Oxygen gas volume contracted when it was subjected to a discharge.
1840	Schönbein	Ozone generation using electrolysis of water, first used the name "ozone" to a peculiar smelling gas
1857	von Siemens	Invention of ozonizer
1860	Andrews and Tait	Coined the terminology "silent discharge"
1865	Soret	Ozone is tri-atomic oxygen (O_3)
1898	Ladenburg	Cold trap to get 86% liquid O_3 with a deep blue color
1892	Otto	Plate-type ozonizer
1902	Warburg	O_3 completely decomposes at 270 °C
1906	Nies (France)	First ozone treatment for drinking water plant
1920	Becker	O_3 formation is determined by specific input energy (P_{dis}/Q_F) rather than voltage, frequency, or flow rate alone.
1943	T. Manley	Discharge power measurement
1979	Rosocha	Coined the name "dielectric barrier discharge"
2021	Bahr El Bakar (Egypt)	World largest wastewater plant (5.6×10^6 m^3 d^{-1}) adopting ozone treatment

Later, Otto developed plate-to-plate type ozonizer [27]. Tesla also worked on ozonizer and patented the use of his high-frequency discharge and build the Tesla Ozone Company for ozonizer business [32]. However, the de facto configuration for large scale O_3 generation is still the Siemens type (i.e., cylindrical DBD arrangement) probably due to maintenance issues. Scale-up of this tube-type ozonizer is accomplished by increasing the number of tubes installed in a main vessel. Application of DBD is not limited to ozonizer, but CO_2 lasers [33, 34], display panel [35], mercury-free UV lamp [36, 37], and surface activation.

In contrast to AC-operated coronas (i.e., discharges without a dielectric barrier), the discharge current waveform in DBD has a 90° phase difference due to the presence of a dielectric barrier between the electrodes. DBD is characterized by multiple microdischarges distributed in time and space. Each microdischarge, also called a streamer, has a duration of 10–100 ns and current pulse amplitude in the range of 100 mA, resulting in 10-100 pC of transferred charge and several μJ of discharge energy. As indicated by Eliason and Kogelschatz, plate-to-plate DBD with transparent electrodes can capture the spatial distribution of microdischarges and the spreading of the microdischarge channel on the dielectric surface, similar to what is obtained in so-called Lichtenberg figures [15]. The electron density reaches 10^{12}–10^{17} cm^{-3} while the average electron temperature is 1–5 eV.

To characterize the discharge and determine the plasma power for large-scale ozone generators the approach of Manley from 1943 is still sufficient [38]. Modifications on this approach are required for more complicated electrode geometries with non-uniform discharge gaps and edge effects at the electrodes, for surface DBDs and packed bed reactors, pulsed discharge operation, or when single microdischarges or structured discharge regimes need to be described [28, 39, 40]. The simplest electrical equivalent for an ozonizer DBD consists of two capacitances, resembling the barrier and the gas gap (C_d and C_g), respectively. Its linear arrangement results in a total capacitance C_{cell}. The current measured at the DBD always contains a capacitive component with $I_{cap} \propto C_{cell} \times dV/dt$. When the voltage amplitude exceeds the threshold V_{min} the microdischarges appear as individual spikes (at low overvoltage) or form “humps” (at high overvoltage, i.e., many microdischarge current pulses overlap). This discharge activity starts when the gap voltage reaches the discharge or breakdown voltage of the gap and stops at the apexes of the applied voltage (i.e., when $dV/dt = 0$) [41]. A time-dependent current source or a resistor $R(t)$ in parallel to the gap capacitance represents the discharge. Instead of measuring the current, it is recommended to record the charge, as this does not require high bandwidth probes and oscilloscopes. If this is not considered properly for the recording of current waveforms, these signals are not reliable, and can lead to erroneous interpretations. The charge is measured as the voltage drop, V_m, over a measuring capacitor, C_m. To keep this voltage drop small, the value of C_m should be much higher than C_d (rule of thumb: factor 10^3). The typical capacitance of DBD reactors (i.e., C_d) usually takes a value of 100s pF, so the C_m value of 100 nF or higher will be acceptable. Plotting the charge as a function of applied voltage results in a V–Q parallelogram also referred to as Lissajous figures. Its area is the energy per high voltage period T (with repetition frequency $f = 1/T$) and thus, the discharge power (P_{dis}) is determined as given in equation (1).

$$P_{dis} = \frac{1}{T}\int_0^T V(t) \times I(t)dt = fC_m \oint V dV_m \quad (1)$$

Many operating parameters affect the ozone formation. Positive correlation with increasing order is usually observed for applied voltage amplitude, frequency, and pressure (~ 0.3 MPa). On the other hand, negative correlations are well recognized for the discharge gap, humidity, and temperature. Optimization of ozonizer basically depends on the controlling these parameters to their optimum levels. In case of humidity, industrial ozonizer adopts a dew point of about −50 °C (i.e., H_2O < 100 ppm). In many fields of plasma chemistry, the chemical changes are expressed by the ratio of discharge power (P_{dis}) and gas flow rate (Q_F), which is often referred to as many different names: energy density (ED), specific input energy (SIE), and specific energy input (SEI). Rough description often found in literature is that ozone formation increases with applied voltage amplitude, discharge current, gas residence time, and frequency, while gas flow rate has an inverse relation. In 1920, Becker described the ozone formation as a function of P_{dis}/Q_F [42]. As the applied voltage and discharge current or frequency increase, so does the Becker parameter (P_{dis}/Q_F) and, consequently, the ozone formation increase. This correlation has been supported by many independent works for a wide range of gas flow rates [43−45]. It is also true for frequency variation [46, 47], however the deviation becomes prominent because the higher frequency increases the temperature. Jodzis and Barczynski introduced a maximum attainable ozone

concentration ($[O_3]_{max}$) at a given condition and described the final ozone concentration as indicated in the semi-empirical form of Eq. (2) [48].

$$[O_3] = [O_3]_{max}\left(1 - \exp\left(-k_E \frac{P_{dis}}{Q_F}\right)\right) = [O_3]_{max}(1 - \exp(-k_E \cdot SIE)) \quad (2)$$

Here, the k_E represents an energy constant (L J^{-1}) [49]. It is worth noting that the $[O_3]_{max}$ exists for a given condition regardless of the initial O_3 concentration even higher than the $[O_3]_{max}$. In other words, the balance between formation and decomposition of O_3 determines the $[O_3]_{max}$ depending on the back reaction, and temperature or degree of cooling. Back reactions consist of two pathways; thermal decomposition and electron impact dissociation of O_3. Jodzis and Baran highlighted that ozone decomposition is primarily influenced by temperature within the microdischarge channel, rather than the bulk gas temperature in the reactor [50]. Additionally, the electron impact process can also contribute to the reverse reaction (O_3 decomposition), and this is dependent on the mean electron energy and the corresponding cross section [51]. As a consequence, when aiming for high concentration O_3 production, it becomes crucial to carefully manage the electron impact dissociation and consider strategies to minimize its impact on the overall energy efficiency. Kitayama and Kuzumoto suggested that operation of DBD under high electric field can suppress the decomposition of ozone by reducing low-energy electrons responsible for the O_3 decomposition [52]. Understanding these processes is vital for a comprehensive understanding of ozone dynamics and its decomposition reactions.

Fig. 3 summarizes ozone formation trends in air and O_2 which have been reported by many different groups. In the air-fed ozonizer, O_3 formation increases linearly with SIE. However, at higher SIE an ozone poisoning mode appears where NO_x catalytically decomposes O_3 and a rapid drop of outlet O_3 concentration happens [53, 54]. The O_2-fed ozonizer usually produces 2~4 times higher O_3 concentration than air, which is also reported in the literature [55−57].

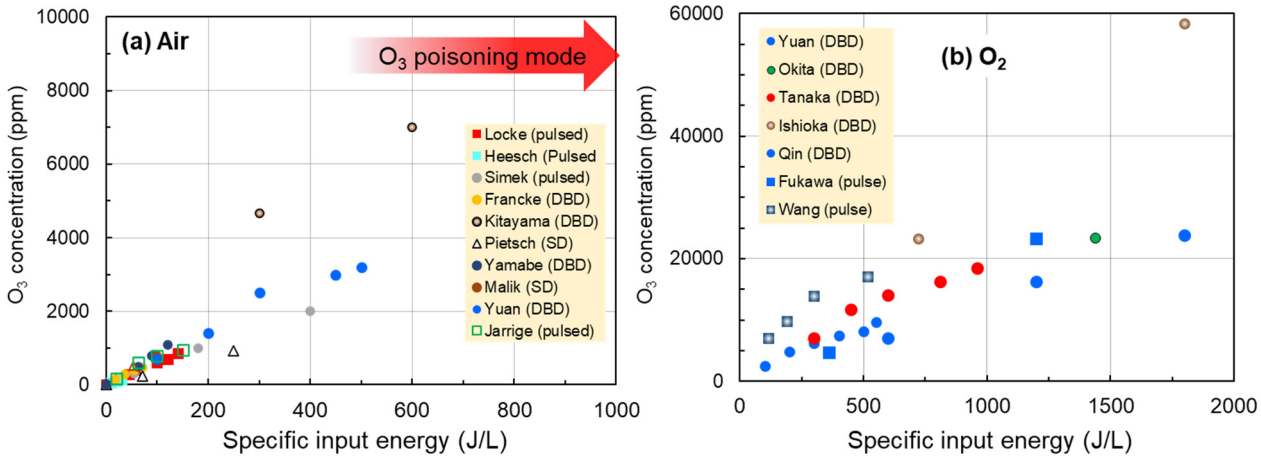

Fig. 3. Ozone formation in different reactors and different conditions: (a) Data for air-fed ozonizer [43, 51, 56, 58-64] (b) data for O_2-fed ozonizer [57, 62, 65-68].

Gap distance in DBD plays an important role in determining the efficiency. For an extreme case, commercial ozonizer adopts gap distance as small as 100s μm with elevated pressure [51, 69]. Hayakawa *et al*. used DBD with 250 μm gap distance for CO_2 decomposition [44, 54, 70]. The narrow discharge gap intensifies the electric field, suppressing the production of low-energy electrons, which benefits ozone production in O_2-fed reactors. Moreover, as the ozone formation process is a three-body collision, the ozone production rate increases with increasing gas pressure at narrow gaps. Modifying the volume-to-surface ratio by reducing the gap may enhance the effective cooling of DBD, which is favorable for ozone generation. Another design concept, commonly referred as the "intelligent gap design" attempts a tailored degree of filamentation (number and strength of microdischarges) in the discharge tube. Therefore, the overall discharge tube consists of four segments with different discharge gap and thus microdischarge properties. In the first segment, strong microdischarges are generated while the subsequent segments employ weaker microdischarges in order to minimize the reactions leading to O_3 decomposition [71]. Nanosecond pulsed

discharge can be used for efficient ozone generation, as it can be operated at higher flow rates without increasing pressure drop along the reactor compared with the narrow gap DBD [72−75]. Fukawa *et al.* investigated nanosecond pulse discharge and obtained maximum ozone concentration of 57 g Nm^{-3} and maximum yield of 900 g kWh^{-1} [66] which is superior to the narrow gap DBD ozonizer.

The presence of small voids between the electrodes and the dielectric produces the so-called "parasitic (or parasitic) discharge", which occurs at the external region of the effective discharge volume. As illustrated in Fig. 4, these parasite discharges are prone to form at both edges of outer electrode and the microvoid between the ground electrode and dielectric material. Since the parasite discharge does not contribute to chemical reaction, it leads to an overestimation of the effective power, and thus an underestimation of energy efficiency regardless of reaction type [28, 114]. One possible way to eliminate the parasite discharge is to use conducting liquid electrodes or spray coating of electrodes and cover both edges by a dielectric material. The careful design can provide complete contact between the dielectric and electrodes confining the discharge areas only in the gaps where the feeding gas is passing through.

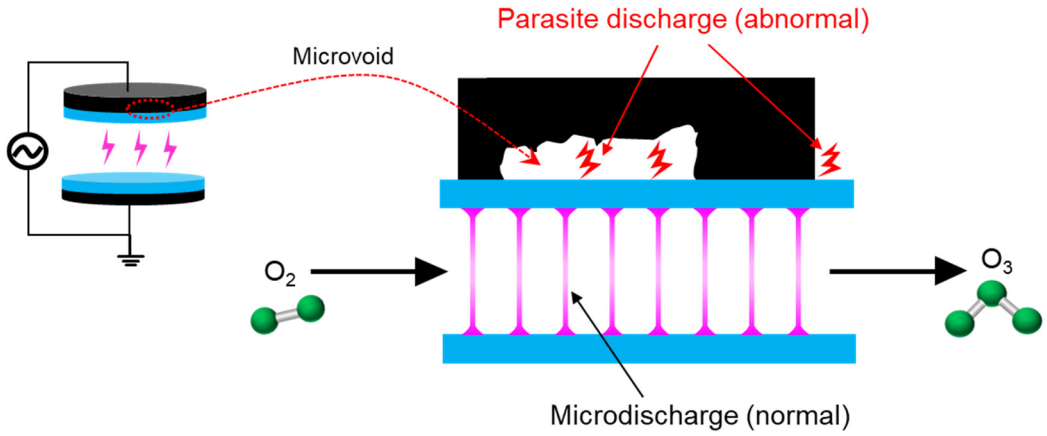

Fig. 4. Schematic illustration of parasite discharge in DBD reactor.

Dielectric materials have a crucial role in controlling the general behavior of the DBD reactors, and one significant factor is surface conductivity. Modifying the surface conductivity of materials, such as alumina, can greatly enhance the uniformity and stability of discharge. For instance, coating alumina with ZnO drastically changed the surface conductivity from ~10^{14} Ω cm^{-1} to 10^{8} Ω cm^{-1} and led to significant improvements in the performance of the DBD reactor [76]. A similar observation was also reported for O_2-fed ozonizer when the surface of glass was coated with CrO_3 and $Cr(NO_3)_3$ [68]. They observed an increase of the ozone yield by approximately 20 % when a rust from stainless steel (SUS304) electrode formed on the surface of the glass covering the high voltage electrode. Comparison of Lissajous figures with and without the rust deposition indicated that the electron emission from glass covered electrode was enhanced with the rust deposition. Fine tuning of the discharge parameters such as applied voltage and frequency, could also enable uniform glow-like discharges in air at atmospheric-pressure especially when the alumina barrier was used and it acted as a cathode [77, 78]. DBD plasma is also widely used in plasma catalysis where the catalysts are placed directly within the plasma zone (i.e., DBD reactor) or downstream of the DBD reactor. The position of catalyst divides the type of reactors into single-stage and two-stage [79]. Recently, DBD coupled with fluidized-bed reactor is the subject of increasing attentions in plasma catalysis, because of its effective interaction between plasma and the surface of catalyst [80–81]. The nonthermal nature of DBD can mitigate the severe heat stress of catalyst that can leads to the longer lifetime with high activity [82]. The influence of packing materials on the discharge properties has also intensively studied both in experiment [83−85] and modeling [86−89]. The details of DBD oriented for plasma catalysis are available in many excellent review papers and references there in [80, 85, 90−92], and will not be discussed further here.

The ozone zero phenomenon (OZP) is a recently recognized problematic feature in DBD where the outlet ozone concentration drops down to zero even without any discharge failure [93]. This phenomenon is particularly observed when high purity oxygen (> 99.9999%) is used for ozone precursor. Interestingly, there are no significant changes in the discharge current and formation of O atoms, as confirmed by its optical

emission at 777 nm, even after the starting of OZP, indicating that alterations in plasma dynamics are not the main cause of this behavior. Operating the DBD at higher power density (0.25 W cm^{-2}) seems to promote the appearance of OZP compared to the low power densities (0.04 W cm^{-2}) [66]. Once OZP is developed in a specific DBD reactor, it can catalytically decompose ozone even without the presence of plasma. While temporarily feeding air, N_2 or H_2O can recover the capability of O_3 formation, the OZP appears again as the feeding gas is switched back to high-purity O_2. Overcoming the OZP will require concerted efforts and collaborations across various disciplines, including physicochemical aspect of plasma chemistry and material science. Understanding the underlying mechanisms and developing in-situ/operando measurement of the surface will be key steps towards addressing this challenge. Further research and cooperation among experts in the field will be crucial to finding effective solutions and advancing DBD technology for ozone generation and its related applications.

2.3 Applications of ozone

Two important common features in all types of ozone applications are low working temperature (no heat stress) and no residues after the treatment. Unlike other chemical treatments such as chlorine, O_3 simply returns to oxygen without leaving residual substances. Fundamental behavior of ozone has been studied intensively for chemical properties [94], catalytic decomposition [94], thermal decomposition [95], cross sections for electron impact [96], and reaction rate coefficient [97, 98] and please refer the details in literature. Fig. 5 classifies the applications of ozone into four categories. Considering the long history of ozonizer, sporadic but unique applications have been tested in early times [1].

The industrial application of ozonizer has been primarily led by water purification for drinking water [99, 100]. The first-ever ozone treatment for drinking water was built in 1893 at Oudshoorn, Netherland. In early 20^{th} century, the number of drinking water plants installing ozonizers exceed 100 in France alone. However, limitation of available electricity during the World War I and II has limited ozone application which eventually led to decrease in the number of plants. The advent of environmental pollution and sustainability shed light on ozonation again. Chlorination is a simple and cost-effective chemical method for water disinfection by damaging cell membrane of microorganisms [101]. The key components for disinfection in chlorination are hypochlorous acid (HOCl) and hypochlorite ions (OCl^-), which possesses high oxidation potential. It also has a long residence time in water after chlorination which enables the long-distance transportation via pipeline. However, chlorination of water containing organic compounds (i.e., humic acid) can be problematic due to the formation of harmful byproducts such as trihalomethanes (THMs), which are known as carcinogenic. Nissinen *et al.* found that chloroform ($CHCl_3$), di- and trichloroacetic acids were the major byproducts in water treatment plants with chlorination [102]. According to the 2022 guidelines for drinking-water quality by the World Health Organization (WHO), the health risk of byproducts in chlorination is considered to be small [103] because regular monitoring of these compounds is required in most countries. Ozone treatment can be alternative to chlorination because it can decompose pollutants dissolved in water and inactivates microorganisms as well [104, 105]. In wastewater treatment, ozone can contribute in many ways, such as increasing dissolved oxygen (DO), reducing BOD (biological oxygen demand), COD (chemical oxygen demand) and TOC (total organic carbon), removing dye (color), reducing sludge formation, providing disinfection, and odor control [106]. The detailed byproducts analysis on the ozone disinfection has also been reported [107]. With the advent of advanced oxidation process (AOP) [108, 109], ozone has been combined with other technologies such as UV, H_2O_2, and electrical discharge plasmas to generate OH radicals on-demand, which have a very high oxidizing potential. It is surprising to see that the Siemens's ozonizer has been used over 160 years without major modifications since its first invention [110]. The global market for ozone technology reached 606 million USD in 2011 in which 76% (460 million USD) for water/wastewater treatment [111]. The world largest wastewater treatment plant using ozone, as of 2021, has a capacity of 5.6×10^6 m^3 d^{-1} which is installed in the Bahr El Bakar facility in Sinai Egypt [112]. The Aqua Aerobic Systems, Inc and Metawater USA operates the largest facility in the Texas USA with a capacity of 800 kg-O_3 h^{-1} [113] providing drinking water for up to 1.6 million customers on a daily basis.

Combination of ozone and catalyst in tandem configuration, referred to as ozone-assisted catalysis (OAC), is one of emerging technologies for the removal of dilute pollutants in gas-phase or liquid phases. In gas removal application, OAC is often considered as one kind of two-stage plasma catalysis where the catalyst bed is located downstream of the plasma reactor [114]. The role of plasma in OAC is confined to produce O_3 by

feeding only pure O_2 or air into the plasma reactor. The O_2-fed ozonizer can completely suppress the formation of NO_x which is difficult in all type of discharge plasmas in air-like mixtures. The potential of OAC has been studied for the removal of various types of VOCs or their mixture [115-118]. It is interesting to note that the effective catalyst for OAC is not always consistent the effective catalysts in thermal catalysis. One clear example on the "activity inversion" was observed for carbon monoxide, CO, removal between OAC and thermal catalysis [119]. The activity order in thermal catalysis at 200 °C was Pd-$LaFeO_3$> Pd-Cu> Pd > Pd-Mn> Pd-Fe> Pd-Ag. However, the Pd-Ag alloy catalyst was found to be best and the Pd-$LaFeO_3$ was the last. An operando high throughput technique for catalytic reaction in OAC has been recently developed [120], and it is expected to promote and accelerate the OAC applications.

Food, seafood, and agriculture are also an important application area of ozone with low-medium concentrations [121−123]. One important characteristic of ozone for food and post-harvest application is that free of heat stress that can possibly damage the quality of product. Ozone is also eco-friendly method in cereal industry to treat seeds without heating [124]. Efficacy of ozone on cereals processing includes microbial decontamination, mycotoxin degradation, insect control, starch modification, functional quality changes, and germination ability. Powerful oxidizing potential of ozone can destroy microorganism which is useful to prevent food poisoning. Bactericidal and antimicrobial effects increase shelf life of various food products and fishes [125−127]. Crowe *et al*. applied aqueous ozone sprays at concentration up to 1.5 mg L^{-1} to improve the microbial safety and quality of salmon fillets [128]. To ensure the food quality during the storage, interaction between ozone ice and food (specifically, lipid, protein, etc.) should be considered. Kinetic analysis of lipid oxidation in ozone-processed shrimp during iced storage showed first-order for lipid oxidation but independent of duration of ozone exposures [129].

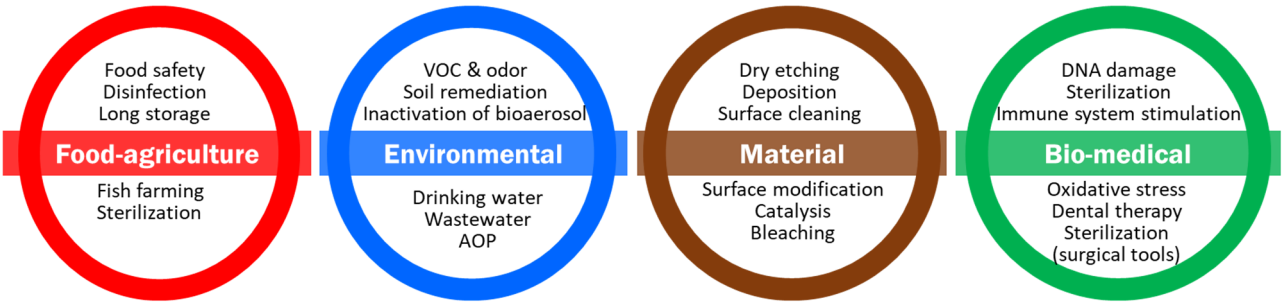

Fig. 5. Application mapping of ozone for four different categories.

Medical application of ozone is one of interesting areas which dates back to 1900s and is increasingly being used in various areas such as orthopedics, cutaneous, and mucosal infections as well as in dentistry [130, 131]. Recently, ozone therapy has been verified in peripheral blood circulation disorder, inflammation, cancer, chronic hepatitis and is getting status of new field named "plasma medicine" [132-135]. The ozone injection method varies depending on the specific target and area being treated. For instance, ozone water has been utilized for treating skin conditions. Additionally, gas-phase ozone injection, including subcutaneous, intra-articular, and arterial injections, is also a viable method to directly administer ozone to the targeted area. Similar to the other medical drugs, the balance between the health benefits and side effect should be considered based on the injection dose [130]. Human body contains a lot of antioxidants including uric acid, ascorbic acid, cysteine, glutathione, albumin, GSH redox system, NADPH and superoxide dismutase (SOD). These antioxidants extend the working range of O_3 dose without deleterious side effects. Ozone is proven to have antimicrobial, insecticidal, and mycotoxin degradation effects. This strong oxidizing power of ozone can substitute harmful chemicals such as chloroform, ethylene oxide which benefit both patient and clinic environment. Saturated oils such sesame, sunflower, and olive oils can extend the lifetime of ozone [136]. Valacchi *et al*. applied ozonated sesame oil for wound healing and found higher wound closure rate with moderate ozone dose (peroxide value about 1500) [137]. Of course, the beneficial and adverse effect of ozone treatment depends on the dose or exposure time [138]. Recently, Roth *et al*. reported wearable ozone-based antibiotic therapy system for treating bacterial infection on the human skin [139]. Various specified studies have been also reported sporadically for the interaction between ozone and cholesterol [140]. Rapid progress in understanding the influence and the chemistry ozone in living cell on a level of DNA damage will bring huge impact on the bio-medical field.

2.4 Long-term storage of ozone

Plasma ozone production is considered as an environmentally friendly and sustainable process, mainly because the plasma reactor can be powered by electricity derived from renewable energy sources. Additionally, owing to ozone's inherent instability, on-demand and on-site production and utilization have become the standard practice in ozone utilization. This decentralized approach to ozone production brings significant environmental benefits, particularly since transportation is a major contributor to CO_2 emissions. Moreover, preserving unstable ozone for extended periods (weeks or months) can enhance compatibility with intermittent renewable energy sources. In this review, we introduce three important approaches shown in Fig. 6 to preserve ozone for long periods: ozone cylinder, ozonated water, and ozone ice. The first interesting approach involves using a pressurized O_3 gas cylinder, similar to other gas cylinder products. Two essential components to achieve this are the choice of appropriate materials and maintain a low temperature. The gas cylinder made of stainless steel requires surface passive treatment to render it inert to O_3. Ozone produced from an O_2-fed ozonizer is initially concentrated to 50% using adsorption and desorption methods. Subsequently, it is exposed to the target surface at room temperature for the passivation treatment of gas cylinder [141]. When the O_3 gas cylinder is stored at 0 °C, the initial concentration of 5% does not decrease over a period of 3 months. However, when the temperature was increased to 25 °C, the ozone concentration decreased by half. This decrease is attributed to the thermal instability of O_3, as discussed earlier. Ozone tends to decompose more rapidly at higher temperatures, which is why it is crucial to preserve the gas cylinder at lower temperatures to maintain its ozone content for an extended period. The second approach is dissolving gas-phase ozone into water, which can extend the life-time of ozone. Ozone can be transferred from gas to liquid using two methods: either by passing an ozone-containing gas through a diffuser into the liquid or by directly applying plasma in contact with water [142]. The use of microbubble has also been extensively tested to increase the dissolution of ozone by increasing the effective contacting time [143]. Ozone has moderate solubility, and its maximum concentration in liquid depends on factors such as temperature [144], pH, and the presence of coexisting substances [145].

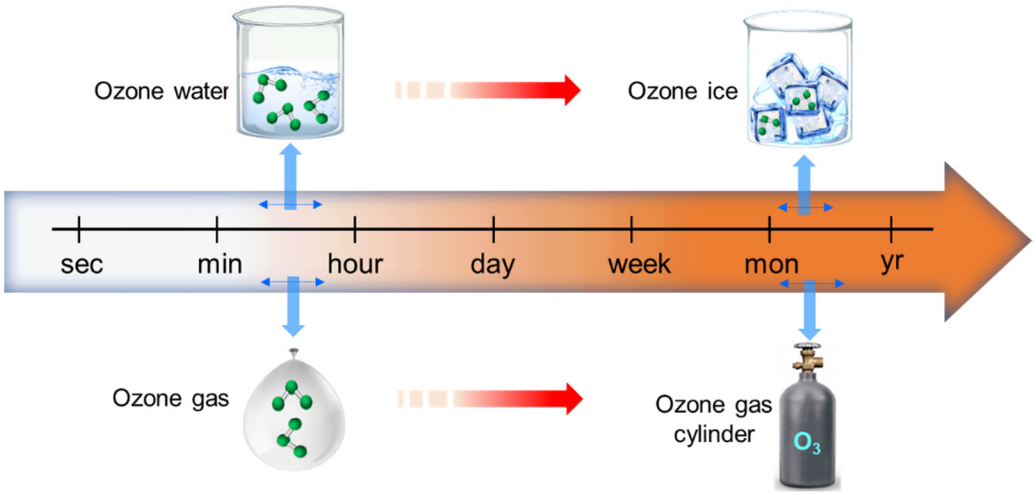

Fig. 6. Preservation of ozone for extended use.

Ozone ice has proven to be a simple and effective method for the long-term preservation of O_3. It is simply prepared by freezing ozonated water. Micro bubble containing ozone has also been tested to increase ozone content in the ice [146]. Although ozone loss occurs during the freezing and melting processes, this approach allows for the separation of the time and space of O_3 production from its usages. The concentration of ozone n the ozone-ice or slurry typically ranges from 0.1 to 0.5 mg L^{-1} [101]. Centralized mass production can be a cost-saving and efficient approach, just like in other manufacturing processes, and it can be applicable to ozone ice production. The decay of ozone proceeds rapidly in the first 2-3 hours, depending on its initial concentration, but then remains relatively constant over the following days [147]. It is speculated that higher ozone concentration is distributed at the surface of ozone ice and radially escape to gas phase depending on the perturbation to the surface. Campos *et al*. reported that using ozonized slurry ice resulted in longer shelf life for the storage of sardine compared to normal slurry ice [148]. Another promising method for maintaining high

ozone concentrations is through clathrate hydrate, where ozone can be kept at a mole fraction of 0.9% after a 20-day storage at −25 °C at 3 MPa [149].

3. Nonequilibrium and thermodynamic limit

3.1 Direction of chemical reaction

Thermodynamics provides a useful insight into chemical reaction in terms of spontaneity and direction. The Gibbs free energy can predict the direction of the chemical reaction, as long as temperature and pressure remain constant. If a reaction is endergonic, i.e. $\Delta G > 0$ (ΔG is defined by enthalpy, temperature, and entropy; $\Delta G = \Delta H - T\Delta S$), it is nonspontaneous. Despite the long history and numerous publications on DBD ozonizers over the past century, there have been limited studies on the thermodynamic considerations [150]. Fig. 7 illustrates the reaction coordinate of O_3 formation process in oxygen. Ozone formation from O_2 (R1) is an endothermic process (ΔH = 142.7 kJ mol^{-1}) which requires energy input to convert O_2 to O_3.

$$3O_2 \rightarrow 2O_3 \qquad (\Delta G^0 = 163.2 \text{ kJ mol}^{-1}) \qquad \text{(R1)}$$

In theory, when the temperature increases, the equilibrium between reactant oxygen and product ozone shifts towards ozone due to the endothermic nature of R1. At 3400 K, the equilibrium constant ($K = pO_2{}^3/pO_3{}^2$) reaches its maximum with a maximum concentration in parts per trillion (ppt) level. However, this condition is far from effective ozone generation. In thermal plasma, such as inductively coupled plasma (ICP) torch, the ozone yield is only 2 g kWh^{-1} [151], which is two orders of magnitude smaller than those in nonthermal plasmas [68].

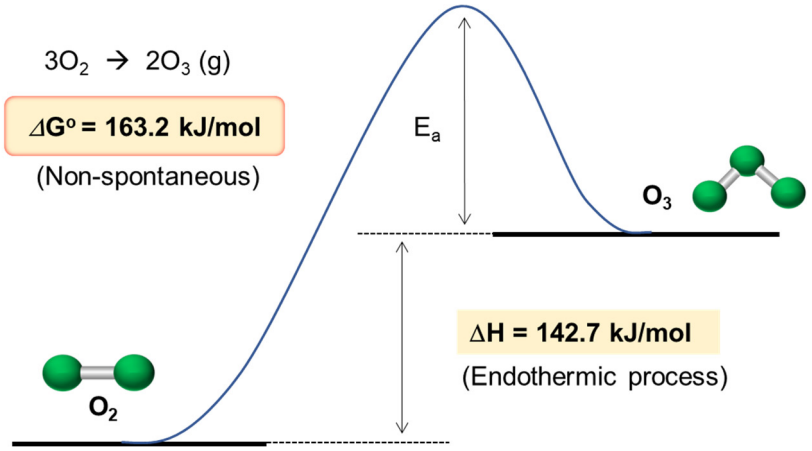

Fig. 7. Reaction diagram of O_3 formation from O_2.

There are two different theoretical maxima of ozone yield in literature. One is 1200 g-O_3 kWh^{-1} derived from the reaction enthalpy (142.7 kJ mol^{-1}) of R1 [51, 152]. Ozone yields obtained in experiments have never exceeded this theoretical maximum and are widely acknowledged by many researchers. However, as will be discussed in the next section, this estimation is too much simplified and does not reflect the actual elementary process. The other theoretical maximum is based on the energy cost of O atom formation assuming that the produced O atom is converted to O_3 without loss [153, 154]. Tabata estimated the energy cost to be 4.35 eV molecule^{-1} for O atom formation at 80 Td, which correspond to the ozone yield of 412 g-O_3 kWh^{-1} [153]. However, if we simply calculate these values using the bond energy of ground state O_2 (5.01 eV), the energy cost of O atom formation and ozone yield would be 2.5 eV molecule^{-1} and 590 g-O_3 kWh^{-1} respectively. Nevertheless, it is essential to note that several experimental studies have reported ozone yields higher than 590 g-O_3 kWh^{-1}. These observations indicate the existence of an oxygen dissociation pathway that requires less energy than the bond energy of ground state O_2.

The Gibbs free energy of R1 is endergonic (ΔG^0 = 163.2 kJ mol^{-1}), indicating that it is a nonspontaneous process. On the other hand, the reverse reaction (O_3 decomposition) is thermodynamically favorable as it is

normally experienced. As the temperature increases, ozone becomes unstable and disappears completely at above 270 °C. This contradictory condition renders O_3 formation difficult under traditional thermochemical process. However, in DBD ozonizers, the reality is completely reversed, and all commercial ozonizers adopt a cooling system despite the endothermic nature of O_3 formation (R1). Indeed, the thermodynamic properties involved in O_3 formation may seem counterintuitive at first glance, making it puzzling for the layman to grasp the concepts of plasma chemistry. However, O_3 formation in DBD is the most widely known example in nonthermal plasma chemistry. The answer to this question will be discussed in the next section.

It should be noted that thermodynamics determines the spontaneity of a given reaction, and the speed of reaction is related to kinetics. For instance, a classic example of exergonic process is changing diamond to graphite ($\Delta G^0 = -2.9$ kJ mol^{-1}; however, this transformation typically does not occur because the reaction rate is too slow. Another similar example is the direct reduction of NO into N_2, which is also exergonic ($\Delta G^0 = -170.6$ kJ mol^{-1}). Although direct NO reduction is feasible from a thermodynamic standpoint, it requires combination of catalyst and chemical reducing agents to realize this reaction, which is referred to as the selective catalytic reduction (SCR) process.

3.2 Coupling non-equilibrium with equilibrium processes

Ozone formation can be divided into two essential elementary steps of O_2 dissociation (R2) and the combination reaction of O_3 (R3). From the Gibbs free energy, it is evident that R2 is highly nonspontaneous, while the second step R3 is a spontaneous process. Fig. 8 depicts how and why nonthermal plasma can successfully generate O_3, defying the thermodynamic limit mentioned above. The key feature lies in the effective coupling of two elementary processes with different time scales and thermodynamic properties. As mentioned in the previous section, the dissociation of O_2 molecules is a highly endothermic process with a reaction enthalpy of 249.2 kJ mol^{-1}. DBD plasma utilizes energetic electrons to dissociate O_2 with a time scale of 10^{-8} s, making this step non-Arrhenius in nature. The dissociation of O_2 is primarily governed by fast electron collision processes (R4 and R5), which depend on the electron energy distribution and the corresponding cross sections. Substituting the highly endothermic step (R2) with energetic electron collision processes (R4 and R4) is the key aspect of how nonthermal plasma overturns the entire process. The actual elementary step for O_3 formation (R3) is an exothermal and exergonic process, occurring spontaneously. The reaction rate constant of R3 is highly temperature-dependent ($k = 8 \times 10^{-12} \exp(-2060/T)$: cm^3 molecule^{-1} s^{-1}), following the Arrhenius process. As mentioned in Section 2.2, electron impact process can indeed contribute to ozone decomposition via R6, and this can have implications on the energy yield for high concentration O_3 generation. When high concentrations of ozone are being generated, the presence of electron impact dissociation can lead to an increase in the reverse reaction (O_3 decomposition), reducing the overall energy efficiency of the ozone generation process.

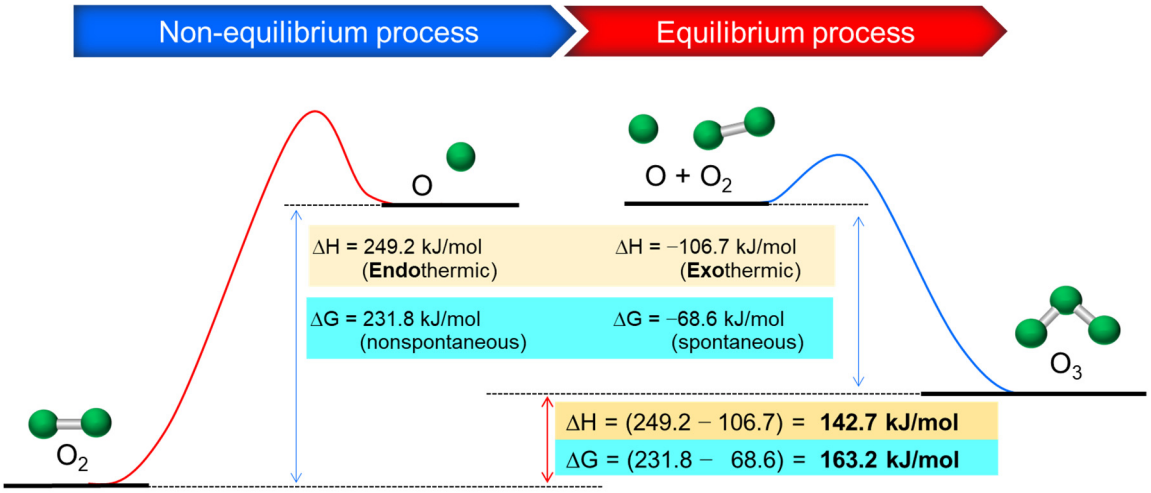

Fig. 8. Coupling of non-equilibrium and equilibrium processes for O_3 formation in plasma. Substituting the highly endothermic process by a highly energetic electron impact process is the crux of DBD (nonthermal plasma) for O_3 generation.

In reality, gas heating in DBD originates not only from the heat of reaction (ΔH of R3) but also from the plasma itself via Joule heating and dielectric loss. The cooling device in commercial DBD is directly related to R3 and heating by plasma. The reaction rate of R3 also depends on the O_2 partial pressure, making the time constant smaller in pure O_2 compared to that in air. Time-resolved UV absorption imaging provided detailed insight on the dynamics of O_3 formation after the streamer inception. In pure oxygen, ozone formation completes within 10−20 μs after the streamer, which is in good agreement with the experimental and simulation results [15, 74, 155−157]. In an air-fed ozonizer, the time constant was found to be approximately 30 ~ 90 μs, consistent with both experiment [158−160] and simulation [157, 161]. The time scale of the reaction is much shorter than the typical gas residence time (10^{-1} ~ 10^{0} s), making the DBD primarily depends on Becker parameter (P_{dis}/Q_F) rather than gas residence time. TALIF and other UV absorption measurements confirmed that the decay of O atom correlates with the O_3 formation [162].

$$O_2 \rightarrow 2O \qquad (\Delta G^0 = 231.8 \text{ kJ mol}^{-1}) \tag{R2}$$

$$O + O_2 \rightarrow O_3 \qquad (\Delta G^0 = -68.6 \text{ kJ mol}^{-1}) \tag{R3}$$

$$O_2 + e \rightarrow O(^3P) + O(^3P) + e \tag{R4}$$

$$O_2 + e \rightarrow O(^3P) + O(^1D) + e \tag{R5}$$

$$O_3 + e \rightarrow O(^1D) + O_2 + e \tag{R6}$$

Threshold energy for O_2 dissociation is 5.1 eV (492.0 kJ mol^{-1}), while dissociative attachment (R7) occurs with an electron energy of 3.6 eV (347.3 kJ mol^{-1}) [163]. Vibrationally excited oxygen molecules, often referred to as hot oxygen, can influence the process by altering the threshold energy and cross section [164]. Spence and Schulz demonstrated a reduction in the onset of O^- production from 4.4 eV at 300 K to 3.5 eV at 1000 K [165]. Even more, Lacombe *et al*. reported 3.5 ± 0.2 eV of threshold electron energy for O_3 formation at 30 K over a multilayer O_2 condensed on metal surfaces under high vacuum [166]. Ono and Oda used two-dimensional UV absorption with pulsed laser to measure ozone distribution and found that ozone is mostly concentrated in the secondary streamer channel [167]. They also speculated that the high temperature and vibrational excitation of O_2 ($v > 1$) could contribute to the dominant O_3 formation in the secondary streamer region. These observations and literature suggest the possibility of achieving one-step higher ozone generation by actively utilizing vibrationally excited oxygen molecules. However, DBD ozonizer with frequency higher than 100 kHz remains a technical curiosity and requires further exploration.

$$O_2 + e \rightarrow O + O^- + e \tag{R7}$$

$$k = Ae^{\left(-\frac{E_a}{RT}\right)} \tag{3}$$

$$k_e = \int f(e)(2e/m)^{\frac{1}{2}}\sigma(e)de \tag{4}$$

Table 3 provides a summary of the thermodynamic properties involved in the ozone formation process. As indicated in R4–R5, the dissociation of oxygen is the initial and crucial step in the ozone formation pathway. This process is primarily controlled by energetic electrons with a typical time scale of ~ 10^{-8} s, which corresponds to the duration of streamer or microdischarge. The distribution of electron energy in DBD plasma is not governed by thermal equilibrium but by the reduced electric field, leading to a highly non-equilibrium state. These electronic processes (R4–R5) effectively replace the highly endothermic reaction of R2, allowing the first step of O_3 formation to proceed even at room temperature. The unique coupling of these different processes in the DBD reactor allows for the successful generation of ozone despite the thermodynamic limitations.

Table 3. Thermodynamic properties of ozone formation process.

Reaction	O formation (R2)	O_3 formation (R3)
Key player	Electron-molecule collision	Atom-molecule recombination
Heat of reaction (ΔH)	Endothermic ($\Delta H > 0$) (249.2 kJ mol^{-1})	Exothermic ($\Delta H < 0$) (−106.7 kJ mol^{-1})
Gibbs free energy (ΔG)	Endergonic Non-spontaneous ($\Delta G > 0$) (231.8 kJ mol^{-1})	Exergonic Spontaneous ($\Delta G < 0$) (− 68.6 kJ mol^{-1})
Time scale	~ 10^{-8} s	~ 10^{-4} s
Governing factor of reaction rate constant	Electron temperature (T_e)	Gas temperature (T_g)
Reaction classification	Non-Arrhenius type	Arrhenius type
Reaction rate constant	$k_e = \int f(\epsilon)(2e/m)^{\frac{1}{2}}\sigma(\epsilon)d\epsilon$	$k = Ae^{(-\frac{E_a}{RT})}$

4. Conclusion

In this brief review, we provided a short overview of the history of ozonizer, starting from the time of von Siemens up to recent years. We briefly described the typical configuration of DBD and general behavior in ozone generation. Recent progress in ozone application was also explained based on the four categories of food-agriculture, environmental, material, and bio-medical fields. The primary concern of this review is to provide retrospect on the distinctive characteristics of thermodynamics in ozone generation which seems to be against the thermodynamic limit at first glance. We explained how a DBD ozonizer connects two independent endothermic and exothermic processes with different time scales, allowing for the endothermic process even at low temperature conditions. By utilizing energetic electron-driven processes, the highly endothermic process transformed into a quasi-exothermic process which can proceed spontaneously. The energetic electrons generated in the non-equilibrium plasma state facilitate the endothermic dissociation of oxygen molecules, compensating for the thermodynamic barriers, and leading to the exothermic formation of ozone. We also suggest that active utilization of vibrationally excited O_2 could be an interesting way for the next generation ozonizer.

Acknowledgment

This work was partly supported by JST CREST (grant number: JPMJCR19R3).

References

[1] Rubin M. B., The history of ozone. The Schonbein Period, 1839-1868, *Bull. Hist. Chem.*, Vol. 26 (1), pp. 40−56, 2001.
[2] Kogelschatz U., Dielectric-barrier discharges: their history, discharge physics, and industrial applications, *Plasma Chem. Plasma Proc.*, Vol. 23 (1), pp. 1−46, 2003.
[3] Molina M. J. and Rowland F. S., Stratospheric sink for chlorofluoromethanes: chlorine atom-catalysed destruction of ozone, *Nature*, Vol. 249, pp. 810–812, 1974.
[4] Boelter K. J. and Davidson J. H., Ozone generation by indoor electrostatic air cleaners, *Aerosol Sci. Technol.*, Vol. 27, pp. 689−708, 1997.
[5] Moreau E., Souakri S., Bellanger R., and Benard N., Ionic wind produced by a millimeter-gap DC corona discharge ignited between a plate and an inclined needle, *Int. J. Plasma Environ. Sci. Technol.*, Vol. 15 (1), e01001, 2021.

[6] Touchard G., Plasma actuators for aeronautics applications- State of art review, *Int. J. Plasma Environ. Sci. Technol.*, Vol. 2 (1), pp. 1−25, 2008.
[7] Tirumala R., Benard N., Moreau E., Fenot M., Lalizel G., and Dorignac E., Temperature characterization of dielectric barrier discharge actuators: influence of electrical and geometric parameters, *J. Phys. D: Appl. Phys.*, Vol. 47 (25), 255203, 2014.
[8] Epelle E. I., Macfarlane A., Cusack M., Burns A., Okolie J. A., Mackay W., Rateb M., and Yaseen M., Ozone application in different industries: A review of recent developments, *Chem. Eng. J.*, Vol. 454, 140188, 2023.
[9] Pratt A., Graziosi P., Bergenti I., Prezioso M., Dediu A., and Yamauchi Y., Ultrahigh vacuum and low-temperature cleaning of oxide surfaces using a low-concentration ozone beam, *Rev. Sci. Instrum.*, Vol. 85 (7), 075116, 2014.
[10] Xu J., Zhang C., Shao T., Fang Z., and Yan P., Formation of hydrophobic coating on PMMA surface using unipolar nanosecond-pulse DBD in atmospheric air, *J. Electrostat.*, Vol. 71 (3), pp. 435−439, 2013.
[11] Borcia G., Anderson C. A., and Brown N. M. D., Using a nitrogen dielectric barrier discharge for surface treatment, *Plasma Source Sci. Technol.*, Vol. 14 (2), pp. 259−267, 2005.
[12] Suzuki R. O., Ogawa T., and Ono K., Use of ozone to prepare silver oxides, *J. Am. Ceram. Soc*, Vol. 82 (8), pp. 2033−2038, 1999.
[13] Menard L. D., Xu F., Nuzzo R. G., and Yang J. C., Preparation of TiO_2-supported Au nanoparticle catalysts from a Au_{13} cluster precursor: Ligand removal using ozone exposure versus a rapid thermal treatment, *J. Catal.*, Vol. 243, pp. 64−73, 2006.
[14] Eliasson B. and Kogelschatz U., Electron impact dissociation in oxygen, *J. Phys. B: At. Mol. Opt. Phys.*, Vol. 19 (8), pp. 1241−1247, 1986.
[15] Eliasson B., Hirth M., and Kogelschatz U., Ozone synthesis from oxygen in dielectric barrier discharges, *J. Phys. D: Appl. Phys.*, Vol. 20 (11), pp. 1421−1437, 1987.
[16] Eliasson B. and Kogelschatz U., Modeling and applications of silent discharge plasmas, *IEEE Trans. Plasma Sci.*, Vol. 19 (2), pp. 309−323, 1991.
[17] Kozlov K. V., Wagner H.-E., Brandenburg R., and Michel P., Spactio temporally resolved spectroscopic diagnostics of the barrier discharge in air at atmospheric pressure, *J. Phys. D: Appl. Phys.*, Vol. 34 (21), pp. 3164−3176, 2001.
[18] Wagner H. E., Brandenburg R., Kozlov K. V., Sonnenfeld A., Michel P., and Behnke J. F., The barrier discharge: basic properties and applications to surface treatment, *Vacuum*, Vol. 71, pp. 417−436, 2003.
[19] *Werner von Siemens A brimming Spirit*: Murmann publishers, 2016.
[20] *Werner von Siemens*. Munich, 2008.
[21] Bähr J., "Lifelines - Werner von Siemens " Simens Historical Institute Berlin 2016.
[22] Spinks J. W. T. and Woods R. J., *An introduction to radiation chemistry*, Thrid Ed. ed: John Wiley & Sons, Inc, 1990.
[23] Thanos J. C. G., Fritz H. P., and Wabner D., The influences of the electrolyte and the physical conditions on ozone production by the electrolysis of water, *J. Appl. Electrochem.*, Vol. 14, pp. 389−399, 1984.
[24] Stucki S., Theis G., Kotz R., H.Devantay, and Christen H. J., In situ production of ozone in water using a membrel electrolyzer, *J. Electrochem. Soc.*, Vol., pp. 367−371, 1985.
[25] Anderegg F. O., Chemical reactions in the corona. 1. Ozone formation, *J. Am. Chem. Soc.*, Vol. 39 (12), pp. 2581−2595, 1917.
[26] Otto W. H. and Bennett W. H., Ozone in silent electric discharge, *J. Chem. Phys.*, Vol. 8 (12), pp. 899−903, 1940.
[27] Horvath M., Bilitzky L., and Huttner J., *Topics in inorganic and general chemistry; Ozone*, Vol. 20. Amsterdam: Elsevier, 1985.
[28] Brandenburg R., Dielectric barrier discharges: progress on plasma sources and on the understanding of regimes and single filaments, *Plasma Sources Sci. Technol.*, Vol. 26 (5), 053001, 2017.
[29] Rosocha L. A., Design and analysis of transient high-voltage electrical devices: Ozone production in fast pulsed dielectric barrier discharges in oxygen and modeling of an intense relativistic electron beam source, Ph.D Dissertation, The University of Wisconsin-Madison, 1979.
[30] Samojlovich G., Gibalov V. I., and Kozlov K. V., *Physical chemistry of the barrier discharge*, 2nd Ed. ed. Düsseldorf: : DVS-Verlag GmbH, 1997.
[31] Pavlovskaya E. N., Podmoshenskii I. V., and Yakovleva A. V., Barrier discharge radiation with condenser ceramics, *J. Appl. Spectroscopy*, Vol. 20, pp. 383−385, 1974.
[32] Tesla N., Apparatus for producing ozone, 568177 USA Patent, 1896.
[33] Kuzumoto M., Ogawa S., and Yagi S., Role of N_2 gas in a transverse-flow CW CO_2 laser excited by silent discharge, *J. Phys. D: Appl. Phys.*, Vol. 22 (12), pp. 1835−1839, 1989.
[34] Yasui K., Kuzumoto M., Ogawa S., Tanaka M., and Yagi S., Silent discharge excited TEM_{00} 2.5 kW CO_2 laser, *IEEE J. Quantum Electron.*, Vol. 25 (4), pp. 836−840, 1989.
[35] Hagelaar G. J. M., Klein M. H., Snijkers R. J. M. M., and Kroesen G. M. W., Energy loss mechanisms in the microdischarges in plasma display panels, *J. Appl. Phys.*, Vol. 89 (4), pp. 2033−2039, 2001.

[36] Kogelschatz U., Silent discharges for the generation of ultraviolet and vacuum ultraviolet excimer radiation, *Pure & Appl. Chem.*, Vol. 62 (9), pp. 1667−1674, 1990.
[37] Eliasson B. and Gellert B., Investigation of resonance and excimer radiation from a dielectric barrier discharge in mixtures of mercury and the rare gases, *J. Appl. Phys.*, Vol. 68 (5), pp. 2026−2037, 1990.
[38] Manley T. C., The electric characteristics of the ozonator discharge, *Trans. Electrochem. Soc.*, Vol. 84, pp. 83−96, 1943.
[39] Peeters F. J. F. and Sanden M. C. M. v. d., The influence of partial surface discharging on the electrical characterization of DBDs, *Plasma Sources Sci. Technol.*, Vol. 24 (1), 015016, 2015.
[40] Pipa A. V., Hoder T., Koskulics J., Schmidt M., and Brandenburg R., Experimental determination of dielectric barrier discharge capacitance, *Rev. Sci. Instrum.*, Vol. 83 (7), 075111, 2012.
[41] Abdelaziz A. A., Seto T., Abdel-Salam M., and Otani Y., Performance of a surface dielectric barrier discharge based reactor for destruction of naphthalene in an air stream, *J. Phys. D: Appl. Phys.*, Vol. 45 (11), 115201, 2012.
[42] Becker H., Uber die extrapolation und berechnung der konzentration und ausbeute von ozonapparaten, *Veroffentl Siemens-Konzern*, Vol. 1, pp. 76−106, 1920.
[43] Simek M. and Clupek M., Efficiency of ozone production by pulsed positive corona discharge in synthetic air, *J. Phys. D: Appl. Phys.*, Vol. 35 (11), pp. 1171−1175, 2002.
[44] Yagi S. and Tanaka M., Mechanism of ozone generation in air-fed ozonisers, *J. Phys. D: Appl. Phys.*, Vol. 12 (9), pp. 1509−1520, 1979.
[45] Yamatake A., Yasuoka K., and Ishii S., Ozone generation by a DC driven micro-hollow cathode discharge in nitrogen-mixed oxygen flow, *Jpn. J. Appl. Phys.*, Vol. 43 (9A), pp. 6381−6384, 2004.
[46] Simek M., Pekarek S., and Prukner V., Influence of power modulation on ozone production using an AC surface dielectric barrierdischarge in oxygen, *Plasma Chem. Plasma Proc.*, Vol. 30, pp. 607−617, 2010.
[47] Abdelaziz A. A., Ishijima T., Seto T., Osawa N., Wedaa H., and Otani Y., Characterization of surface dielectric barrier discharge influenced by intermediate frequency for ozone production, *Plasma Source Sci. Technol.*, Vol. 25 (3), 035012, 2016.
[48] Jodzis S. and Barczynski T., Ozone synthesis and decomposition in oxygen-fed pulsed DBD system: effect of ozone concentration, power density, and residence time, *Ozone Sci. Eng.*, Vol. 41 (1), pp. 69−79, 2019.
[49] Kim H. H., Prieto G., Takashima K., Katsura S., and Mizuno A., Performance evaluation of discharge plasma process for gaseous pollutant removal, *J. Electrostat.*, Vol. 55, pp. 25−41, 2002.
[50] Jodzis S. and Baran K., The influence of gas temperature on ozone generation and decomposition in ozone generator. How is ozone decomposed?, *Vacuum*, Vol. 195, pp. 110647, 2022.
[51] Kitayama J. and Kuzumoto M., Analysis of ozone generation from air in silent discharge, *J. Phys. D: Appl. Phys.*, Vol. 32 (23), pp. 3032−3040, 1999.
[52] Kitayama J. and Kuzumoto M., Theoretical and experimental study on ozone generation characteristics of an oxygen-fed ozone generator in silent discharge, *J. Phys. D: Appl. Phys.*, Vol. 30, pp. 2453−2461, 1997.
[53] Donohoe K. G., Shair F. H., and Wulf O. R., Production of O_3, NO, and N_2O in a pulsed discharge at 1 atm, *Ind. Eng. Chem. Fundam.*, Vol. 16 (2), pp. 208−215, 1977.
[54] Yagi S., Tanaka M., and Tabata N., Generation of NO_x in ozonizer, *Trans. IEE Japan*, Vol. 99 (5/6), pp. 41−48, 1979.
[55] Robinson J. A., Bergougnou M. A., Cairns W. L., Castle G. S. P., and Inculet I. I., A new type of ozone generator using taylor cones on water surfaces, *IEEE Trans. Ind. Applicat.*, Vol. 34 (6), pp. 1218−1224, 1998.
[56] Pietsch G. J. and Gibalov V. I., Dielectric barrier discharges and ozone synthesis, *Pure & Appl. Chem.*, Vol. 70 (6), pp. 1169−1174, 1998.
[57] Wang D., Matsumoto T., Namihira T., and Akiyama H., Development of higher yield ozonizer based on nano-seconds pulsed discharge *J. Adv. Oxid. Technol.*, Vol. 13 (1), pp. 71−78, 2010.
[58] Locke B. R., Ichihashi A., Kim H. H., and Mizuno A., Diesel engine exhaust treatment with a pulsed streamer corona reactor equipped with reticulated vitreous carbon electrodes, *IEEE Trans. Ind. Applicat.*, Vol. 37 (3), pp. 715−723, 2001.
[59] Heesch E. J. M. v., Winands G. J. J., and Pemen A. J. M., Evaluation of pulsed streamer corona experiments to determine the O* radical yield, *J. Phys. D: Appl. Phys.*, Vol. 41 (23), 234015, 2008.
[60] Francke K. P., Rudolph R., and Miessner H., Design and operation characteristics of a simple and reliable DBD reactor for use with atmospheric air, *Plasma Chem. Plasma Proc.*, Vol. 23 (1), pp. 47−57, 2003.
[61] Malik M. A. and Hughes D., Ozone synthesis improves by increasing number density of plasma channels and lower voltage in a nonthermal plasma, *J. Phys. D: Appl. Phys.*, Vol. 49 (13), 135202, 2016.
[62] Yuan D., Wang Z., Ding C., He Y., Whiddon R., and Cen K., Ozone production in parallel multichannel dielectric barrier discharge from oxygen and air: the influence of gas pressure, *J. Phys. D: Appl. Phys.*, Vol. 49 (45), 455203, 2016.
[63] Jarrige J. and Vervisch P., Plasma-enhanced catalysis of propane and isopropyl alcohol at ambient temperature on a MnO_2-based catalyst, *Appl. Catal. B: Environ.*, Vol. 90, pp. 74−82, 2009.

[64] Cieplak T., Yamabe C., Ihara S., Satoh S., and Cieplak J., The effect of electrode rotation on the ozone generation process, *Trans. IEE Japan*, Vol. 119 (7), pp. 925−930, 1999.
[65] Ishioka H., Toraguchi M., Nishii H., and Yamabe C., High concentration ozone generation by micro gap silent discharge, *Trans. IEE Japan*, Vol. 122 (4), pp. 378−383, 2002 (in Japanese).
[66] Fukawa F., Taguchi M., Suzuki S., and Itoh H., Ozone production characteristics in a dielectric barrier discharge type ozonizer, *IEEJ Trans. FM*, Vol. 133 (9), pp. 471−477, 2013 (in Japanese).
[67] Qin Y., Qian S., Wang C., and Xia W., Effects of nitrogen on ozone synthesis in packed-bed dielectric barrier discharge, *Plasma Sci. Technol.*, Vol. 20 (9), 095501, 2018.
[68] Tanaka M., Ogawa S., Wada N., Yoshiyasu H., and Yagi S., Influence of rust on electrodes of oxygen-fed ozonizer to ozone generation, *IEEJ Trans. FM*, Vol. 125, pp. 817−822, 2005 (in Japanese).
[69] Kuzumoto M., Tabata Y., Yoshizawa K., and Yagi S., High density ozone generation by silent discharge under extremely short gap length around 100 μm, *Trans. IEE Japan*, Vol. 116 (2), pp. 127−127, 1996 (in Japanese).
[70] Hayakawa Y., Emeraldi P., Imai T., and Kambara S., CO_2 conversion characteristics by micro-gap DBD plasma reactor, *Int. J. Plasma Environ. Sci. Technol.*, Vol. 17 (1), e01007, 2023.
[71] Lopez J., "Progress in large-scale ozone generation using microplasmas," in *Complex Plasmas.*, Bonitz, M., Lopez, J., Becker, K., Thomsen, H. , Ed. Heidelberg: Springer, 2014.
[72] Vahid F. and Howarth C. R., Synthesis of ozone in dielectricless discharges, *Chem. Eng. J.*, Vol. 32 (1), pp. 43−51, 1986.
[73] Masuda S., Sato M., and Seki T., High efficiency ozonizer using traveling wave pulse voltage, *IEEE Trans. Ind. Applicat.*, Vol. 22 (5), pp. 886−891, 1986.
[74] Nilsson J. O. and Eninger J. E., Numerical modeling of ozone production in a pulsed homogeneous discharge: A parameter study, *IEEE Trans. Plasma Sci.*, Vol. 25 (1), pp. 73−82, 1997.
[75] Wang D. and Namihira T., Nanosecond pulsed streamer discharges: II. Physics, discharge characterization and plasma processing, *Plasma Source Sci. Technol.*, Vol. 29 (2), 023001, 2020.
[76] Choi J. H., Lee T. I., Han I. H., Oh B. Y., Jeong M. C., Myoung J. M., and Baik H. K., Improvement of plasma uniformity using ZnO-coated dielectric barrier discharge in open air, *Appl. Phys. Lett.*, Vol. 89, 081501, 2006.
[77] Osawa N. and Yoshioka Y., Generation of low-frequency homogeneous dielectric barrier discharge at atmospheric pressure, *IEEE Trans. Plasma Sci.*, Vol. 40 (1), pp. 2−8, 2012.
[78] Osawa N., Yoshioka Y., Hanaoka R., Mochizuki Y., Kobayashi Y., and Yamada Y., Generation of uniform discharge by dielectric barrier discharge device in atmospheric-pressure air, *Electrical Eng. Jpn.*, Vol. 180 (4), pp. 1−9, 2012.
[79] Kim H. H., Teramoto Y., Negishi N., and Ogata A., A multidisciplinary approach to understand the interactions of nonthermal plasma and catalyst: A review, *Catal. Today*, Vol. 256, pp. 13−22, 2015.
[80] Chen X., Kim H.-H., and Nozaki T., Plasma catalytic technology for CH_4 and CO_2 conversion: A review highlighting fluidized-bed plasma reactor, *Plasma Process. Polym.*, Vol. 20, e2200207, 2023.
[81] Kim D.-Y., Ham H., Chen X., Liu S., Xu H., Lu B., Furukawa S., Kim H.-H., Takakusagi S., Sasaki K., and Nozaki T., Cooperative catalysis of vibrationally excited CO_2 and alloy catalyst breaks the thermodynamic equilibrium limitation, *J. Am. Chem. Soc.*, Vol. 144 (31), pp. 14140−14149, 2022.
[82] Zhan C., Kim D.-Y., Xu S., Kim H.-H., and Nozaki T., Nonthermal plasma catalysis of CO_2 methanation over multi-metallic Ru based catalysts, *Int. J. Plasma Environ. Sci. Technol.*, Vol. 16 (3), e03006, 2022.
[83] Butterworth T. and Allen R. W. K., Plasma-catalyst interaction studied in a single pellet DBD reactor: dielectric constant effect on plasma dynamics, *Plasma Sources Sci. Technol.*, Vol. 26 (6), 065008, 2017.
[84] Mei D., Zhu X., He Y.-L., Yan J. D., and Tu X., Plasma-assisted conversion of CO_2 in a dielectric barrier discharge reactor: understanding the effect of packing materials, *Plasma Source Sci. Technol.*, Vol. 24 (1), 015001, 2014.
[85] Kim H. H., Teramoto Y., Ogata A., Kang W. S., Hur M., and Song Y.-H., Negative surface streamers propagating on TiO_2 and γ-Al_2O_3-supported Ag catalysts: ICCD imaging and modeling study, *J. Phys. D: Appl. Phys.*, Vol. 51 (24), 244006, 2018.
[86] Kang W. S., Kim H.-H., Teramoto Y., Ogata A., Lee J. Y., Kim D.-W., Hur M., and Song Y.-H., Surface streamer propagations on an alumina bead: experimental observation and numerical modeling, *Plasma Sources Sci. Technol.*, Vol. 27 (1), 015018, 2018.
[87] Kruszelnicki J., Engeling K. W., Foster J. E., Xiong Z., and Kushner M. J., Propagation of negative electrical discharges through 2-dimensional packed bed reactors, *J. Phys. D: Appl. Phys.*, Vol. 50 (2), 025203, 2017.
[88] Kruszelnicki J., Ma R., and Kushner M. J., Propagation of atmospheric pressure plasmas through interconnected pores in dielectric materials, *J. Appl. Phys.*, Vol. 129 (14), 143302, 2021.
[89] Wang W., Kim H. H., Laer K. V., and Bogaerts A., Streamer propagation in a packed bed plasma reactor for plasma catalysis applications, *Chem. Eng. Journal*, Vol. 334, pp. 2467−2479, 2018.
[90] Bogaerts A., Tu X., Whitehead J. C., Centi G., Lefferts L., Guaitella O., Azzolina-Jury F., Kim H.-H., Murphy A. B., Schneider W. F., Nozaki T., Hicks J. C., Rousseau A., Thevenet F., Khacef A., and Carreon M., The 2020 plasma catalysis roadmap, *J. Phys. D: Appl. Phys.*, Vol. 53 (44), 443001, 2020.

[91] Nozaki T. and Okazaki K., Non-thermal plasma catalysis of methane: Principles, energy efficiency, and applications, *Catal. Today*, Vol. 211, pp. 29−38, 2013.
[92] Kim H.-H., Abdelaziz A. A., Teramoto Y., Nozaki T., Hensel K., Mok Y.-S., Saud S., Nguyen D. B., Lee D. H., and Kang W. S., Interim report of plasma catalysis: Footprints in the past and blueprints for the future, *Int. J. Plasma Environ. Sci. Technol.*, Vol. 15 (1), e01004, 2021.
[93] Taguchi M., Yamashiro K., Kakano T., and Itoh H., Extreme decrease of ozone product using high pure oxygen, *Plasma Process. Polym.*, Vol. 4, pp. 719−727, 2007.
[94] Oyama S. T., Chemical and catalytic properties of ozone, *Catal. Rev. Sci. Eng.*, Vol. 42 (3), pp. 279−322, 2000.
[95] Sigmund J., Catalytic destruction of ozone: A cost effective approach to controlling off-gas ozone emissions, *Water Conditioning & Purification*, Vol. (March), pp. 50−53, 2001.
[96] Rangwala S. A., Kumar S. V. K., Krishnakumar E., and Mason N. J., Cross sections for the dissociative electron attachment to ozone, *J. Phys. B: At. Mol. Opt. Phys.*, Vol. 32, pp. 3795−3804, 1999.
[97] Suzuki S., Rusinov I. M., Teranishi K., Shimomura N., and Itoh H., Re-evaluation of rate coefficients for ozone decomposition by oxygen in wide range of gas pressures (20–1000 Torr) and temperatures (293–423 K), *J. Phys. D: Appl. Phys.*, Vol. 51 (30), 305201, 2018.
[98] Guenther J., Krankowsky D., and Mauersberger K., Third-body dependence of rate coefficients for ozone formation in ^{16}O-^{18}O mixtures, *Chem. Phys. Lett*, Vol. 324, pp. 31−36, 2000.
[99] Glaze W. H., Drinking-water treatment with ozone, *Environ. Sci. Technol.*, Vol. 21 (3), pp. 224−230, 1987.
[100] Sonntag C. v. and Gunten U. v., *Chemistry of ozone in water and wastewater treatment: From basic principles to applications*: IWA Publishing, 2020.
[101] Bono G., Okpala C. O. R., Vitale S., Ferrantelli V., Noto A. D., Costa A., Bella C. D., and Monaco D. L., Effects of different ozonized slurry-ice treatments and superchilling storage (−1°C) on microbial spoilage of two important pelagic fish species, *Food Sci. Nutr.*, Vol. 5, pp. 1049−1056, 2017.
[102] Nissinen T. K., Miettinen I. T., Martikainen P. J., and Vartiainen T., Disinfection by-products in Finnish drinking waters, *Chemosphere*, Vol. 48, pp. 9−20, 2002.
[103] *Guidelines for drinking-water quality*, Fourth edition ed. Geneva: World Health Organization, 2022.
[104] Gould J. P. and Jr. W. J. W., Oxidation of phenols by ozone, *J. WPCF*, Vol. 48 (1), pp. 47−60, 1976.
[105] Hoigne J. and Bader H., Ozonation of water: Kinetics of oxidation of ammonia by ozone and hydroxyl radicals, *Environ. Sci. Technol.*, Vol. 12 (1), pp. 79−84, 1978.
[106] Rosen H. M., Use of ozone and oxygen in advanced wastewater treatment, *Water Pollution Control Federation*, Vol. 45 (12), pp. 2521−2536, 1973.
[107] Richardson S. D., Jr. A. D. T., Caughran T. V., Chen P. H., Collette T. W., Floyd T. L., Schenck K. M., Jr. B. W. L., Sun G., and Majetich G., Identification of new ozone disinfection byproducts in drinking water, *Environ. Sci. Technol.*, Vol. 33, pp. 3368−3377, 1999.
[108] Martins A. F., Advanced oxidation processes applied to effluent streams from an agrochemical industry, *Pure & Appl. Chem.*, Vol. 70 (12), pp. 2271−2279, 1998.
[109] Locke B. R., Sato M., Sunka P., Hoffmann M. R., and Chang J. S., Electrohydraulic discharge and nonthermal plasma for water treatment, *Ind. Eng. Chem. Res.*, Vol. 45, pp. 882−905, 2006.
[110] Vosmaer A., *Ozone; its manufacture, properties and uses*. New York: D. Van Nostrand company, 1916.
[111] "Ozone generation: Technologies, markets and players,"Research, B., 2012.
[112] World's largest wastewater treatment plant gears up with innovative ABB technology, https://new.abb.com/news/detail/83095/worlds-largest-wastewater-treatment-plant-gears-up-with-innovative-abb-technology, 13 July 2023.
[113] Drinking water plant is world's largest ozone installation, https://www.waterworld.com/drinking-water/treatment/article/16191858/drinking-water-plant-is-worlds-largest-ozone-installation, 19 July, 2023.
[114] Kim H. H., Nonthermal plasma processing for air pollution control: A historical review, current issues, and future prospects, *Plasma Process. Polym.*, Vol. 1 (2), pp. 91−110, 2004.
[115] Einaga H. and Futamura S., Catalytic oxidation of benzene with ozone over alumina-supported manganese oxides, *J. Catal.*, Vol. 227, pp. 304−312, 2004.
[116] Oh S. M., Kim H. H., Einaga H., Ogata A., Futamura S., and Park D. W., Zeolite-combined plasma reactor for decomposition of toluene, *Thin Solid Films*, Vol. 506−507, pp. 418−422, 2006.
[117] Konova P., Stoyanova M., Naydenov A., Christoskova S., and Mehandjiev D., Catalytic oxidation of VOCs and CO by ozone over alumina supported cobalt oxide, *Appl. Catal. A: Gen.*, Vol. 298, pp. 109−114, 2006.
[118] Gervasini A., Vezzoli G., and Ragaini V., VOC removal by synergic effect of combustion catalyst and ozone, *Catal. Today*, Vol. 29, pp. 449−455, 1996.
[119] Tou A., Kim H. H., Einaga H., Teramoto Y., and Ogata A., Ozone-assisted catalysis of CO: In situ Fourier transform IR evidence of the cooperative effect of a bimetallic Ag-Pd catalyst, *Chem. Eng. J.*, Vol. 355, pp. 380−389, 2019.

[120] Abdelaziz A. A., Teramoto Y., Nozaki T., and Kim H.-H., Operando infrared imaging of ozone-assisted catalysis for high-throughput screening of catalytic activity, *Appl. Catal. A: Gen.*, Vol. 644, 118843, 2022.
[121] Guzzon R., Franciosi E., Moser S., Carafa I., and Larcher R., Application of ozone during grape drying for the production of straw wine. Effects on the microbiota and compositive profile of grapes, *J. Appl. Microbiol.*, Vol. 125 (2), pp. 513−527, 2018.
[122] Sarron E., Gadonna-Widehem P., and Aussenac T., Ozone treatments for preserving fresh vegetables quality: A critical review, *Foods*, Vol. 10 (3), 605, 2021.
[123] Gonçalves A. A., Ozone as a safe and environmentally friendly tool for the seafood industry, *J. Aquatic Food Product Technol.*, Vol. 25 (2), pp. 210−229, 2016.
[124] Sivaranjani S., Prasath V. A., Pandiselvam R., Kothakota A., and Mousavi Khaneghah A., Recent advances in applications of ozone in the cereal industry, *LWT- Food Sci. Technol.*, Vol. 146, 111412, 2021.
[125] Rice R. G., Farquhar J. W., and Bollyky L. J., Review of the applications of ozone for increasing storage times of perishable foods, *Ozone Sci. Eng.*, Vol. 4, pp. 147−163, 1982.
[126] Lu F., Liu S. L., Liu R., Ding Y. C., and Ding Y. T., Combined effect of ozonized water pretreatment and ozonized flake ice on maintaining quality of japanese sea bass (*Lateolabrax japonicus*), *J. Aquatic Food Product Technol.*, Vol. 21, pp. 168−180, 2012.
[127] Blogoslawski W. J. and Stewart M. E., Some ozone applications in seafood, *Ozone Sci. Eng.*, Vol. 33 (5), pp. 368−373, 2011.
[128] Crowe K. M., Skonberg D., Bushway A., and Baxter S., Application of ozone sprays as a strategy to improve the microbial safety and quality of salmon fillets, *Food Control*, Vol. 25 (2), pp. 464−468, 2012.
[129] Okpala C. O. R., Bono G., Geraci M. L., Sardo G., Vitale S., and Schaschke C. J., Lipid oxidation kinetics of ozone-processed shrimp during iced storage using peroxide value measurements, *Food Biosci.*, Vol. 16, pp. 5−10, 2016.
[130] Bocci V., Borrelli E., Travagli V., and Zanardi I., The ozone paradox: Ozone is a strong oxidant as well as a medical drug, *Medicinal Res. Rev.*, Vol. 29 (4), pp. 646−682, 2009.
[131] Somiya I., *New- New technology in ozone utilization (Ozonriyouno Sinngizyutu)*: Sanyusyobo, 1993.
[132] Fridman G., Friedman G., Gutsol A., Anatoly B. Shekhter, Vasilets V. N., and Fridman A., Applied plasma medicine, *Plasma Process. Polym.*, Vol. 5 (6), pp. 503−533, 2008.
[133] Laroussi M., Low-temperature plasma for medicine?, *IEEE Trans. Plasma Sci.*, Vol. 37 (6), pp. 714−725, 2009.
[134] Woedtke T. v., Reuter S., Masur K., and Weltmann K. D., Plasmas for medicine, *Phys. Reports*, Vol. 530, pp. 291−320, 2013.
[135] Bekeschus S., Favia P., Robert E., and Woedtke T. v., White paper on plasma for medicine and hygiene: Future in plasma health sciences, *Plasma Process. Polym.*, Vol. 16 (18), 1800033, 2019.
[136] Hernández F., Hernández D., Zamora Z., Díaz M., Ancheta O., Rodriguez S., and Torres D., *Giardia duodenalis*: Effects of an ozonized sunflower oil product (Oleozon)on in vitro trophozoites, *Exp. Parasitol.*, Vol. 121, pp. 208−212, 2009.
[137] Valacchi G., Lim Y., Belmonte G., Miracco C., Zanardi I., Bocci V., and Travagli V., Ozonated sesame oil enhances cutaneous wound healing in SKH1 mice, *Wound Repair Regeneration*, Vol. 19 (1), pp. 107−115, 2010.
[138] Valacchi G., Fortino V., and Bocci V., The dual action of ozone on the skin, *Brit. J. Dermatology*, Vol., pp. 1096−1100, 2005.
[139] Roth A., Maruthamuthu M. K., Nejati S., Krishnakumar A., Selvamani V., Sedaghat S., Nguyen J., Seleem M. N., and Rahimi R., Wearable adjunct ozone and antibiotic therapy system for treatment of Gram-negative dermal bacterial infection, *Sci. Rep.*, Vol. 12 (1), 13927, 2022.
[140] Gumulka J. and Smith L. L., Ozonization of cholesterol, *J. Am. Chem. Soc.*, Vol. 105 (7), pp. 1972−1979, 1983.
[141] Koike K., Nakamura S., Makihira N., Izumi K., and Takatori S., Method of concentrating ozone gas and apparatus therefor, WO2010010610A1, 2010.
[142] Kuraica M. M., Obradovic B. M., Manojlovic D., Ostojic D. R., and Puric J., Ozonized water generator based on coaxial dielectric-barrier discharge in air, *Vacuum*, Vol. 73, pp. 705−708, 2004.
[143] Takahashi M., Ishikawa H., Asano T., and Horibe H., Effect of microbubbles on ozonized water for photoresist removal, *J. Phys. Chem. C*, Vol. 116 (23), pp. 12578−12583, 2012.
[144] Smedt F. D., Gendt S. D., Heyns M. M., and Vinckier C., The application of ozone in semiconductor cleaning processes: The solubility issue, *J. Electrochem. Soc.*, Vol. 148 (9), pp. G487−G493, 2001.
[145] Gurol M. D. and Akata A., Kinetics of ozone photolysis in aqueous solution, *AIChE J.*, Vol. 42 (11), pp. 3238−3292, 1996.
[146] Matsumoto K., Sameshima K., Teraoka Y., Furuya K., Murahashi K., Hayashi K., and Shirai D., Formation of ozone ice by freezing water containing ozone micro-bubbles: investigation into the influence of surfactant on characteristics of ice containing oxygen micro-bubbles, *Int. J. Refrigeration*, Vol. 36 (3), pp. 842−851, 2013.
[147] Liu Z., Kou J., Xing Y., Sun C., Liu P., and Zhang Y., Ozone Ice as an oxygen release reagent for heap leaching of gold ore, *Minerals*, Vol. 11 (11), 1251, 2021.

[148] Campos C. A., Rodríguez O., Losada V., Aubourg S. P., and Barros-Velázquez J., Effects of storage in ozonised slurry ice on the sensory and microbial quality of sardine (Sardina pilchardus), *Int. J. Food Microbiol.*, Vol. 103 (2), pp. 121−130, 2005.
[149] Nakajima T., Kudo T., Ohmura R., Takeya S., and Mori Y., Molecular storage of ozone in a clathrate hydrate: an attempt at preserving ozone at high concentrations, *PLOS One*, Vol. 7 (11), e48563, 2012.
[150] Ozonek J., Fijalkowski S., and Czerwinski J., Thermodynamic aspects of equilibrium ozone generation, *Plasma Process. Polym.*, Vol. 4, pp. 701−709, 2007.
[151] Stratton B. C., Knight R., Mikkelsen D. R., Blutke A., and Vavruska J., Synthesis of ozone at atmospheric pressure by a quenched induction-coupled plasma torch, *Plasma Chem. Plasma Proc.*, Vol. 19 (2), pp. 191−216, 1999.
[152] Hakiai K., Ihara S., Satoh S., and Yamabe C., Characteristics of ozone generation by a diffuse glow discharge, *T. IEE Japan*, Vol. 117 (12), pp. 1194−1199, 1997 (in Japanese).
[153] Tabata N., Consideration about ozone generation method using electrical discharge, *T. IEE Japan*, Vol. 117 (12), pp. 1200−1206, 1997 (in Japanese).
[154] Kishida H., Ishizaka M., Tanaka Y., Ehara Y., and Ito T., Superposing effect of UV rays on ozone generation by discharge, *T. IEE Japan*, Vol. 117 (6), pp. 585−590, 1997.
[155] Hegeler F. and Akiyama H., Spatial and temporal distributions of ozone after a wire-to-plate streamer discharge, *IEEE Trans. Plasma Sci.*, Vol. 25 (5), pp. 1158−1165, 1997.
[156] Peyrous R., Pignolet P., and Held B., Kinetic simulation of gaseous species created by an electrical discharge in dry or humid oxygen, *J. Phys. D: Appl. Phys.*, Vol. 22 (11), pp. 1658−1667, 1989.
[157] Ikebe K., Nakanishi K., and Arai S., Evolution process of microdischarge products in ozonizer, *IEE of Japan*, Vol. 109 (11), pp. 474−480, 1989 (in Japanese).
[158] Rozoy M., Postel C., and Puech V., NO removal in a photo-triggered discharge reactor, *Plasma Sources Sci. Technol.*, Vol. 8 (3), pp. 337−348, 1999.
[159] Ono R. and Oda T., Dynamics of ozone and OH radicals generated by pulsed corona discharge in humid-air flow reactor measured by laser spectroscopy, *J. Appl. Phys.*, Vol. 93 (10), pp. 5876−5882, 2003.
[160] Ono R. and Oda T., Ozone production process in pulsed positive dielectric barrier discharge, *J. Phys. D: Appl. Phys.*, Vol. 40 (1), pp. 176−182, 2007.
[161] Tapia C. C., Camps E., and Cardoso O. O., Perturbative method for ozone synthesis from oxygen in a single discharge, *IEEE Trans. Plasma Sci.*, Vol. 22 (5), pp. 979−985, 1994.
[162] Shu Z., Qiao J., Wang C., and Xiong Q., Simultaneous quantification of atomic oxygen and ozone by full photo-fragmentation two-photon absorption laser-induced fluorescence spectroscopy, *Plasma Source Sci. Technol.*, Vol. 30 (5), 055001, 2021.
[163] Henderson W. R., Fite W. L., and Brackkmann R. T., Dissociative attachment of electrons to hot oxygen, *Phys. Rev.*, Vol. 183 (1), pp. 157−166, 1969.
[164] O'Malley T. F., Calculation of dissociative attachment in hot O_2, *Phys. Rev.*, Vol. 155 (1), pp. 59−63, 1967.
[165] Spence D. and Schulz G. J., Temperature dependence of dissociative attachment in O_2 and CO_2, *Phys. Rev.*, Vol. 188 (1), pp. 280−287, 1969.
[166] Lacombe S., Cemic F., Jacobi K., Hedhili M. N., Coat Y. L., Azria R., and Tronc M., Electron-induced synthesis of ozone in a dioxygen matrix, *Phys. Rev. Lett.*, Vol. 79 (6), pp. 1146−1149, 1997.
[167] Ono R. and Oda T., Spatial distribution of ozone density in pulsed corona discharges observed by two-dimensional laser absorption method, *J. Phys. D: Appl. Phys.*, Vol. 37 (5), pp. 730−735, 2004.